DTU Library

Improved Focusing Method for 3-D Imaging using Row–Column-Addressed 2-D Arrays

Bouzari, Hamed; Engholm, Mathias; Stuart, Matthias Bo; Thomsen, Erik Vilain; Jensen, Jørgen Arendt

Published in:
Proceedings of the 2017 IEEE International Ultrasonics Symposium (IUS)

Link to article, DOI:
10.1109/ULTSYM.2017.8091596

Publication date:
2017

Document Version
Peer reviewed version

Improved Focusing Method for 3-D Imaging using Row–Column-Addressed 2-D Arrays

Hamed Bouzari*, Mathias Engholm†, Matthias Bo Stuart*, Erik Vilain Thomsen†, and Jørgen Arendt Jensen*
* Center for Fast Ultrasound Imaging, Department of Electrical Engineering, Building 349,
† Department of Micro- and Nanotechnology, Building 344,
Technical University of Denmark, 2800 Kgs. Lyngby, Denmark

***Abstract*—A row–column-addressed (RCA) 2-D array can be interpreted as two orthogonal 1-D arrays. By transmitting with row elements and receiving the echoes through column elements or vice versa, a rectilinear volume in front of the array can be beamformed. Since the transmit and receive 1-D arrays are orthogonal to each other, only one-way focusing is possible in each transmit or receive plane. For applications, where the scatterers are sparse, *e.g.*, in micro-bubble tracking, this study suggests to multiply the envelope data received by the row elements when transmitting with columns as well as the data received by the column elements when transmitting with rows, to improve the focusing. In this way, at each point a two-way focused profile in both transmit and receive directions can be produced. This paper investigates the performance of the new focusing scheme based on simulations and phantom measurements with a PZT $\lambda/2$-pitch 3 MHz 62+62 RCA 2-D transducer probe. A synthetic aperture imaging sequence with single element transmissions at a time, is designed for imaging down to 14 cm at a volume rate of 44 Hz.**

I. Introduction

For ultrasonic 3-D imaging, 2-D array transducers are employed to achieve real-time scanning of a volume [1]–[3]. By arranging the transducer elements in a rectangular grid, it is possible to steer the beam in the lateral and elevation direction and thereby acquire data from a volume. Albeit the principle is simple, in practice it presents a great technical challenge. The number of elements in a fully-addressed (FA) $N \times N$ 2-D array scales with N^2. Addressing each element individually leads to great practical challenges in producing the interconnections from the fabrication point of view, and also in sampling and real-time processing the substantial amount of data.

Alternatively, an $N \times N$ element 2-D array can be operated utilizing only $2N$ connections, when a row–column or cross-electrode addressing scheme is used [4]–[9]. This is contrary to the N^2 connections needed, when conventionally addressing the elements. In general, a row–column-addressed (RCA) array is a 2-D array, which is addressed via its row and column indices. Effectively, this makes two 1-D arrays arranged orthogonal to each other. The limited rectilinear field-of-view, when imaging with these arrays can be overcome by using a curved array. An in-depth study of the possibilities in this approach has been investigated [10], [11].

Another issue with RCA arrays from an imaging perspective is that only one-way focusing is possible in each dimension. This is because the focused lines in transmit and receive are perpendicular to each other. On each transmission with row elements the echoed signals are collected by column elements, thereby beamforming any point in the 3-D region in front of the array. For applications, where the scatterers are sparse, *e.g.*, in micro-bubble tracking, to improve the focusing this study suggests to multiply the envelope data received by the row elements, when transmitting with columns as well as the data received by the column elements when transmitting with rows. By using the proposed method it is possible to achieve two-way focusing in both transmit and receive directions.

II. Focusing with Row-Column Addressed Arrays

The vertical and horizontal arrays of the RCA 2-D array can each steer the transmit ultrasound beam in one direction. When the horizontal array is used as a transmit array, it can steer the transmit angle in the *z*-*x* plane, and at the same time the vertical array is receiving in the *z*-*y* plane. After the sequence has completed, the two arrays switch function, and now the vertical array is used as a transmit array and the horizontal array is receiving. This leads to two identical volumes of the rectilinear region in front of the array. However, at each point only one-way focusing is achievable either in transmit or receive. The pulse-echo pressure fields for both sequences using a rectangular apodization at each point (x,y,z), *i.e.*, $\Phi_{t_R r_C}(x,y,z)$ and $\Phi_{t_C r_R}(x,y,z)$, can be estimated by: [12]

$$\Phi_{t_R r_C}(x,y,z) = \frac{L_y\sqrt{\rho_a}}{\sqrt{\lambda z}} e^{i\frac{\pi}{4}} \operatorname{sinc}\left(\frac{L_y y}{\lambda z}\right) \cdot \frac{L_x\sqrt{\rho_a}}{\sqrt{\lambda z}} e^{i\frac{\pi}{4}} \operatorname{sinc}\left(\frac{L_x x}{\lambda z}\right), \quad (1)$$

$$\Phi_{t_C r_R}(x,y,z) = \frac{L_x\sqrt{\rho_a}}{\sqrt{\lambda z}} e^{i\frac{\pi}{4}} \operatorname{sinc}\left(\frac{L_x x}{\lambda z}\right) \cdot \frac{L_y\sqrt{\rho_a}}{\sqrt{\lambda z}} e^{i\frac{\pi}{4}} \operatorname{sinc}\left(\frac{L_y y}{\lambda z}\right), \quad (2)$$

where L_x and L_y are the length of each row and column element, ρ_a is the mass density of the medium, and λ is the sound wavelength. In a similar way the pulse-echo pressure field for an FA 2-D array can be estimated by:

$$\Phi_{FA}(x,y,z) = \left(\frac{L_y\sqrt{\rho_a}}{\sqrt{\lambda z}} e^{i\frac{\pi}{4}} \operatorname{sinc}\left(\frac{L_y y}{\lambda z}\right) \cdot \frac{L_x\sqrt{\rho_a}}{\sqrt{\lambda z}} e^{i\frac{\pi}{4}} \operatorname{sinc}\left(\frac{L_x x}{\lambda z}\right)\right)^2. \quad (3)$$

The reflected pressure field from the scattering pattern, $\chi(x,y,z)$, using the RCA and FA 2-D arrays, indicated by $P_{t_R r_C}(x,y,z)$, $P_{t_C r_R}(x,y,z)$, and $P_{FA}(x,y,z)$, can be formulated as:

$$P_{t_R r_C}(x,y,z) = \Phi_{t_R r_C}(x,y,z) \underset{t}{*} \chi(x,y,z)\,, \tag{4}$$

$$P_{t_C r_R}(x,y,z) = \Phi_{t_C r_R}(x,y,z) \underset{t}{*} \chi(x,y,z)\,, \tag{5}$$

$$P_{FA}(x,y,z) = \Phi_{FA}(x,y,z) \underset{t}{*} \chi(x,y,z)\,. \tag{6}$$

If the scattering pattern is a point-like target that can be represented as a Dirac function, then:

$$P_{FA}(x,y,z) = P_{t_R r_C}(x,y,z) \cdot P_{t_C r_R}(x,y,z)\,. \tag{7}$$

If the targets are sparse with no overlap within the PSFs, then this also works for a distributed targets. This formula proposes a new method to perform the focusing so that the final spatial resolution is similar to the two-way focusing with fully addressed 2-D arrays. Fig. 1a illustrates the perpendicular transmit and receive focused beam profiles, when transmitting with row elements and receiving the echoes with column elements. On the other hand, if the same transmitting elements were receiving the echoes, as it shown in Fig. 1b for the row elements, a two-way focused profile can be achieved. The two-way focusing in the transmit direction is possible because the transmit and receive focus lines are both in the same plane and therefore the effective aperture squared. Fig. 1b is illustrating the two-way beam profile at the focus line for a situation where row elements transmit and receive the echoes. However, along each focus line it is not known where the scatter was located, as there is no means to focus along each focus line. That is why it is required to use the received RF-data from the perpendicular array to focus along each transmit focal line.

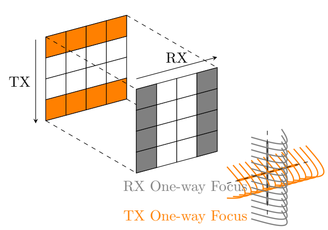

(a) TX rows, RX columns

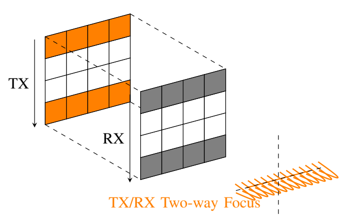

(b) TX/RX rows

Fig. 1. Transmitting and receiving the echoes (a) using both perpendicular 1-D arrays and (b) using one of the 1-D arrays.

III. Methods

A. Synthetic Aperture Imaging Technique

Two synthetic aperture imaging (SAI) sequences were designed for imaging down to 14 cm of depth. They utilize 62 single element transmissions on each row as well as column element. In both sequences the echoes are collected with all the perpendicular elements.

B. Measurement Setup

Measurements are acquired with one prototyped and fully integrated 2-D RCA PZT probe. It is connected to the experimental ultrasound scanner SARUS [13]. The measured RF signals are beamformed using a MATLAB (MathWorks Inc., Massachusetts, USA) implementation of delay-and-sum (DAS) beamformer for RCA 2-D arrays [8]. The transducer's parameters are shown in Table I. For a speed of sound of 1540 m/s, 182 µs is required to acquire a single image line to a depth of 14 cm. For 124 emissions this is equivalent to a volume rate of 44 Hz.

Table I
Transducers' parameters and setup configuration

Center frequency	3	MHz
Pitch row	270	µm
Pitch column	270	µm
Number of rows	62	-
Number of columns	62	-
	SAI sequence	
Frame rate	44	Hz
Pulse repetition frequency	5	kHz
Emissions per frame	124	-
No. of active elements in Tx	1	-
Scan depth (max range)	14	cm
Emission center frequency	3	MHz
Sinusoid emission cycles	2	-
Focus in transmit	0	mm
Focus in receive	Dynamic	-
Tx synthetic electronic apodization	Rect.	-
Rx electronic apodization	Rect.	-
Sampling frequency	70	MHz

A geometrical copper wire phantom, where wires located at different depths with 1 cm spacing, was used as line targets, to evaluate the imaging performance of the proposed focusing method, in terms of FWHM and cystic resolution [11] as a function of depth.

IV. Results

Fig. 2 illustrates three cross planes (Azimuth, Elevation, and C-plane) of the simulated PSFs for different imaging sequences. When using only row elements in transmit and receive, although a two-way focusing is achieved in the elevation plane, no focusing can be made on the lateral plane (Fig. 2.a). Using only column elements for transmit and receive, achieves the same result but on the other perpendicular plane (Fig. 2.b). On the other hand, when using the row elements in transmit and column elements in receive or vice versa, a one-way focusing can be achieved in both lateral and elevation planes (Fig. 2.c and Fig. 2.d). Multiplying the last two PSFs generates a two-way focused PSF in both lateral and elevation planes (Fig. 2.e).

In (7) the reflectivity amplitude of the scatterer can not be preserved, and therefore to account for that, before multiplying the two volumes, each has to be equalized with its maximum value.

Measured examples of the proposed focusing scheme is illustrated in Fig. 3 and Fig. 4. In Fig. 3a and Fig. 4a by transmitting with row elements and receiving the RF-data with column elements a volume in front of the array is imaged. In Fig. 3b and Fig. 4b the proposed method is applied by multiplying the envelope data acquired, when using row elements for transmission and column elements for reception

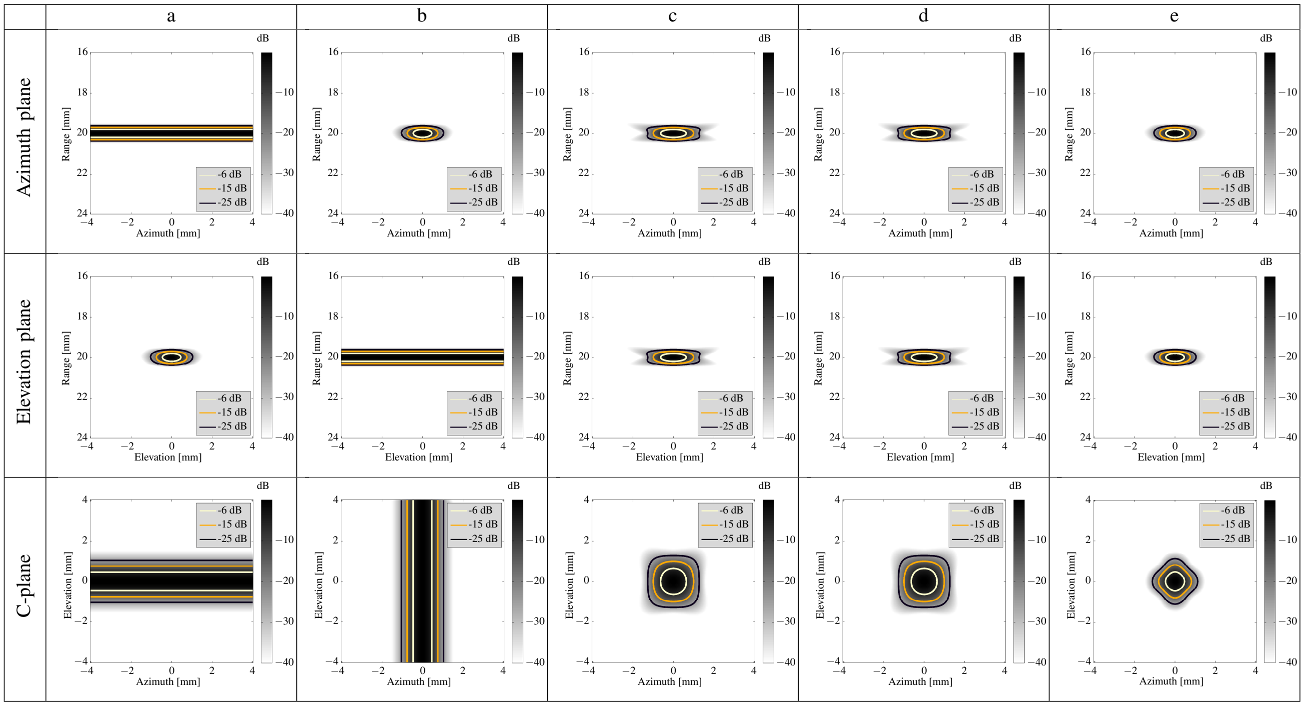

Fig. 2. A scatterer is located at 20 mm depth in front of the array. Three cross planes (Azimuth, Elevation, and C-plane) of the simulated PSFs for different imaging sequences are shown, when: (a) transmitting and receiving with row elements, (b) transmitting and receiving with column elements, (c) transmitting with row and receiving with column elements, (d) transmitting with column and receiving with row elements, and (e) transmitting with both row and column, and receiving with both row and column elements. The C-planes are at depth of 20 mm.

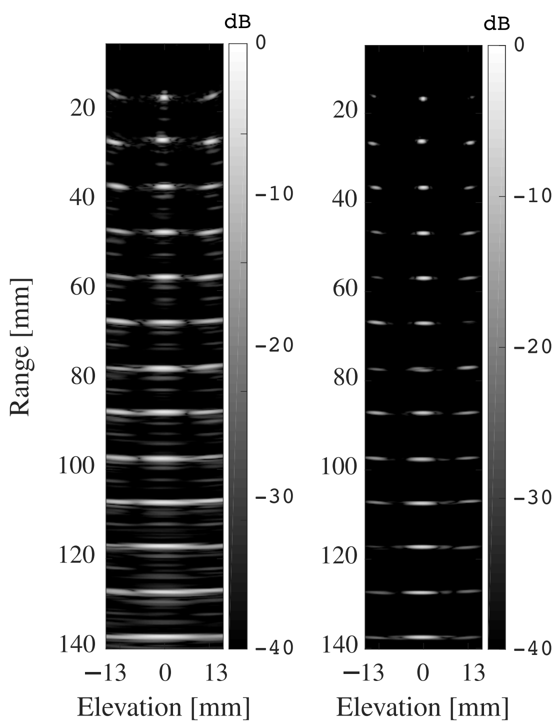

(a) (b)

Fig. 3. Two elevation planes of a wire grid phantom are shown. (a): transmitting with row elements and receiving the RF-data with column elements, (b): the proposed method.

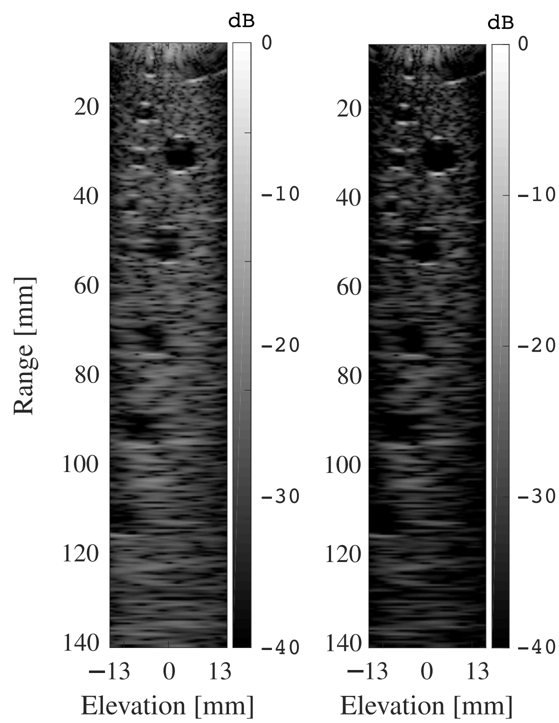

(a) (b)

Fig. 4. Two elevation planes of a hollow cyst phantom are shown. (a): transmitting with row elements and receiving the RF-data with column elements, (b): the proposed method.

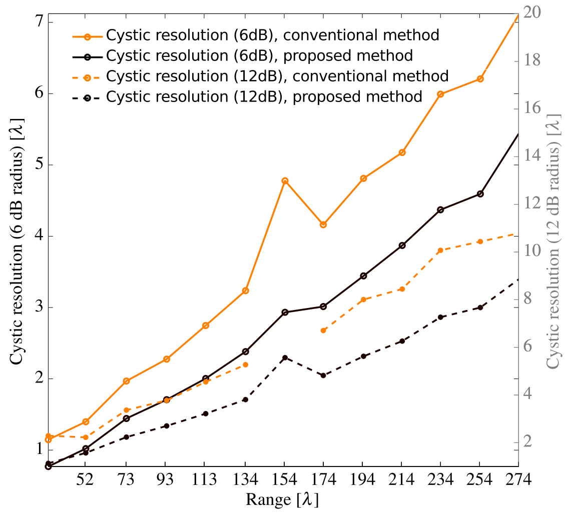

(a) Cystic resolution

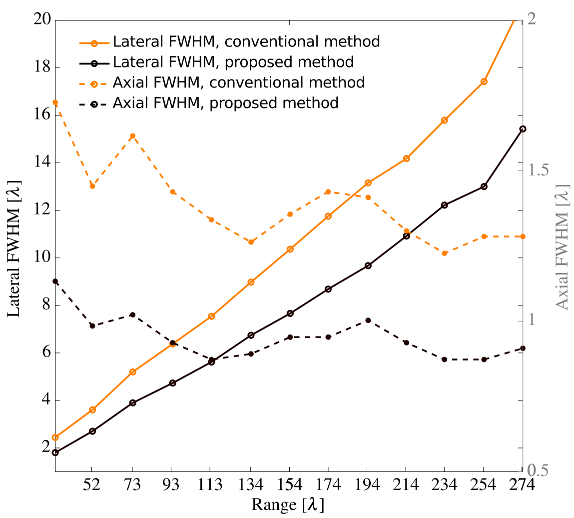

(b) FWHM

Fig. 5. Using the new beamforming method has lowered the FWHM at all depths compared with the normal beamforming method. The echo from the seventh wire has low SNR and therefore its 12dB cystic resolution went to infinity.

and vice versa. The effectiveness of the proposed method is more visible on the wire grid phantom, since the point targets are not overlapping, which is not the case for the cyst phantom. The calculated FWHM and cystic resolution [11], over the middle column of wires, are illustrated in Fig. 5b and Fig. 5a.

Another advantage of the proposed method, is the possibility to lower the number of emissions to acquire a volume. In conventional row–column imaging, in order to have the same spatial resolution in each dimension, we required to transmit with all the transmit elements which is equal to the number of receive elements. However by using the proposed method we do not need necessarily transmit the same number of times as the number of received elements. This is due to the increase in the resolution by using the new method. Therefore, the number of transmissions in each dimension can be decreased.

V. Conclusion

This study presented a method for increasing the spatial resolution of the RCA 2-D arrays and validated it based on simulation and phantom measurements. The proposed method has the limitation to be only applicable to point-like targets, which are distributed sparsely. Compared with the conventional row–column imaging, the proposed method lowers the frame rate, as it requires to acquire each volume region in front of the array two times with the perpendicular 1-D arrays. The method assumes that the scatterers are not moving, however for moving targets a motion compensation method has to be sought. Further study has to be carried out to prove its applicability in ultrasound imaging by tracking micro-bubbles.

References

[1] S. W. Smith, H. G. Pavy, and O. T. von Ramm, "High speed ultrasound volumetric imaging system – Part I: Transducer design and beam steering," *IEEE Trans. Ultrason., Ferroelec., Freq. Contr.*, vol. 38, pp. 100–108, 1991.

[2] O. T. von Ramm, S. W. Smith, and H. G. Pavy, "High speed ultrasound volumetric imaging system – Part II: Parallel processing and image display," *IEEE Trans. Ultrason., Ferroelec., Freq. Contr.*, vol. 38, pp. 109–115, 1991.

[3] D. H. Turnbull and F. S. Foster, "Beam steering with pulsed two-dimensional transducer arrays," *IEEE Trans. Ultrason., Ferroelec., Freq. Contr.*, vol. 38, no. 4, pp. 320–333, July 1991.

[4] C. E. Morton and G. R. Lockwood, "Theoretical assessment of a crossed electrode 2-D array for 3-D imaging," in *Proc. IEEE Ultrason. Symp.*, 2003, pp. 968–971.

[5] C. H. Seo and J. T. Yen, "A 256 x 256 2-D array transducer with row-column addressing for 3-D rectilinear imaging," *IEEE Trans. Ultrason., Ferroelec., Freq. Contr.*, vol. 56, no. 4, pp. 837–847, April 2009.

[6] C. E. M. Démoré, A. Joyce, K. Wall, and G. Lockwood, "Real-time volume imaging using a crossed electrode array," *IEEE Trans. Ultrason., Ferroelec., Freq. Contr.*, vol. 56, no. 6, pp. 1252–1261, 2009.

[7] A. Sampaleanu, P. Zhang, A. Kshirsagar, and R. J. Zemp, "Top-orthogonal-to-bottom electrode (TOBE) 2D CMUT arrays: Towards low-channel-count 3D imaging," jun 2012.

[8] M. F. Rasmussen, T. L. Christiansen, E. V. Thomsen, and J. A. Jensen, "3-D imaging using row–column-addressed arrays with integrated apodization — Part I: Apodization design and line element beamforming," *IEEE Trans. Ultrason., Ferroelec., Freq. Contr.*, vol. 62, no. 5, pp. 947–958, 2015.

[9] R. K. W. Chee, A. Sampaleanu, D. Rishi, and R. J. Zemp, "Top orthogonal to bottom electrode (TOBE) 2-D CMUT arrays for 3-D photoacoustic imaging," *IEEE Trans. Ultrason., Ferroelec., Freq. Contr.*, vol. 61, no. 8, pp. 1393–1395, 2014.

[10] H. Bouzari, M. Engholm, M. B. Stuart, S. I. Nikolov, E. V. Thomsen, and J. A. Jensen, "3-D imaging using row-column-addressed 2-D arrays with a diverging lens," in *Proc. IEEE Ultrason. Symp.*, 2016, pp. 1–4.

[11] H. Bouzari, M. Engholm, C. Beers, M. B. Stuart, S. I. Nikolov, E. V. Thomsen, and J. A. Jensen, "Curvilinear 3-D imaging using row-column-addressed 2-D arrays with a diverging lens: Feasibility study," *IEEE Trans. Ultrason., Ferroelec., Freq. Contr.*, vol. 64, no. 6, pp. 978–988, 2017.

[12] T. L. Szabo, *Diagnostic ultrasound imaging: Inside out*, 2nd ed. Elsevier (Oxford, UK), 2014.

[13] J. A. Jensen, H. Holten-Lund, R. T. Nilsson, M. Hansen, U. D. Larsen, R. P. Domsten, B. G. Tomov, M. B. Stuart, S. I. Nikolov, M. J. Pihl, Y. Du, J. H. Rasmussen, and M. F. Rasmussen, "SARUS: A synthetic aperture real-time ultrasound system," *IEEE Trans. Ultrason., Ferroelec., Freq. Contr.*, vol. 60, no. 9, pp. 1838–1852, 2013.